The Promise of Long-Range Lightning Networks in Storm Analysis and Forecasting

A. Pessi and S. Businger [1], University of Hawaii

K. L. Cummins, University of Arizona

N. W. S. Demetriades and M. Murphy, Vaisala Inc.

Presented at the 88th Annual AMS Meeting in New Orleans, January 2008

1. Introduction

Thunderstorms pose a variety of hazards to aviation and marine interests, including high winds, wind shear, microbursts, turbulence, icing, heavy precipitation, and lightning strikes. In remote regions where conventional weather data are sparse and satellite data are either infrequent or unrevealing, tracking of thunderstorms, squall lines, and developing cyclones are important challenges in weather prediction for civilian and military purposes. The waveguide between the Earth's surface and the ionosphere allows very low frequency (VLF) emissions generated by lightning, called sferics, to propagate over long distances (Fig. 1). The new Pacific Lightning Detection Network (PacNet), as a part of a larger long-range lightning detection network (LLDN), utilizes this attribute to monitor lightning activity over the central North Pacific Ocean with a network of ground-based lightning detectors that have been installed on four widely spaced Pacific islands (400-3800 km) (Fig. 2). PacNet and LLDN sensors combine both magnetic direction finding (MDF) and time-of-arrival (TOA) based technology to locate a strike with as few as two sensors. As a result, the PacNet/LLDN is one of the few observing systems, outside of geostationary satellites, that provide continuous real-time data concerning convective storms throughout a synoptic-scale area over the open ocean. See Pessi et al. (2008) for additional details on the construction and performance of PacNet/LLDN.

Long-range lightning data from PacNet/LLDN are useful not only in planning of trans-oceanic flight routes and in development of optimum ship tracks for ocean voyages, also for assessing the current intensity and near-term potential for intensification in tropical and extratropical cyclones (e.g., Demetriades and Holle, 2005; Futyan and Del Genio, 2007; Squires and Businger 2008). Moreover, relationships between lightning rate and hydrometeors have application over data-sparse ocean regions by allowing lightning-rate data to be used as a proxy for related storm properties, which can be assimilated into NWP models. Finally, case-study results from data assimilation experiments show promising results (Alexander et al 1999; Chang et al. 2001; Papadopoulos et al. 2004; Pessi et al. 2006).

2. Construction of PacNet and assessment of network performance

VLF sensors have been installed on four islands in the North-Pacific Ocean: (i) Unalaska in the Aleutian Islands, Alaska, the Hawaiian Islands of (ii) Hawaii and (iii)

[1] Corresponding author: Department of Meteorology, 2525 Correa Rd., Honolulu, HI 96822. businger@hawaii.edu

Kauai, and (iv) Kwajalein in Marshall Islands (Fig. 3). These sensors work in combination with Vaisala's Long Range Lightning Detection Network (LLDN), which consists of National Lightning Detection Network (NLDN) and Canadian Lightning Detection Network (CLDN) sensors located throughout the U.S. and Canada. The ~200 broadband LF/VLF sensors in these networks are not optimized for long-range detection, but still provide important contributions to the overall network performance. The resulting long-range research network called *PacNet/LLDN* continuously monitors lightning activity associated with convective storms across the central and eastern Pacific Ocean, north of the equator. It is anticipated that additional sites will be added in the future, expanding the network to the western Pacific.

The PacNet sensors[2] are modified IMPACT ESP (Improved Accuracy from Combined Technology, Enhanced Sensitivity and Performance) sensors designed for long-range detection. The gain has been set to a high level in order to receive weak, ionospherically reflected sferics, and the bandwidth has been adjusted to have greatest sensitivity in the VLF band. The sensors use combined technology that employs both time-of-arrival and magnetic direction finding methods in the data processing (Cummins et al. 1998).

For quantitative applications of the PacNet/LLDN data stream, the detection efficiency (DE) and location accuracy (LA) of the network must be assessed, and then an accurate model of these characteristics constructed.

The percentage of lightning flashes reported by long-range lightning detection networks depends on the strength of the lightning discharge, solar angle, the distance between the lightning flashes and the sensors, specifics of the hardware, and the nature of the waveguide, discussed further in Pessi et al. (2008). This flash detection efficiency (DE) is defined as

$$DE(x,y,t) = \frac{\text{number of flashes detected}}{\text{actual number of flashes}} \times 100\% \qquad (1)$$

The detection efficiency and location accuracy of PacNet/LLDN varies with time of the day and the location of the thunderstorm with respect to the sensors. Detection efficiency and location accuracy models have been developed and applied to quantify the lightning rates and locations over the North Pacific region (Pessi et al. 2008). The model parameters were derived by comparing the waveforms arriving at a PacNet test sensor to NLDN lightning data spread throughout the continental United States.

The attenuation rate was derived by time-correlating data from the test sensor with NLDN data collected throughout the U.S., and comparing the lossless signal strength (determined by the NLDN estimated peak current and the known distance) with the peak field strength measured by the test sensor. The analysis of signal strength shows the expected exponential loss in energy with distance (Fig. 4), where the average relative field strength (filled circles) is normalized by the estimated NLDN peak current. The standard deviation error bars show larger errors in the range of 2000-3500 km, where propagation

[2] We hereafter refer the sensors installed on the Pacific islands as "PacNet sensors" and the sensors in North America as "conventional sensors", although PacNet/LLDN is a combination of both.

involves a mix of ground and ionospheric propagation. The daytime attenuation rate shown in Fig. 4a is 10,000 km, and the nighttime attenuation rate is 40,000 km (Fig. 4b).

Lightning data from Puerto Rico were then used in conjunction with LLDN data to derive the salt-water peak current distribution and space constants for the DE model. The results of this effort are shown in Fig. 5. The refined DE model was then applied to the PacNet/LLDN sensor distribution in the central North Pacific (Fig. 2), with the resulting predicted DE distribution shown in Fig. 6. In applying the refined DE model to Hawaii, it is assumed that the weather regime in the two locations, in a prevailing trade-wind belt, will produce similar peak current distributions.

LIS data were used to assess the location accuracy and detection efficiency of PacNet/LLDN. The observed location accuracy was in the range of 13-40 km over the central North Pacific, in reasonable agreement with the LA model. The observed detection efficiency over the central-north region was 17-22% and 40-45% for day and night, respectively. These values were in good agreement with the DE model (Pessi et al. 2008). In the vicinity of Hawaii, the observed DE was 21-23% and 57-61% for day and night, respectively. These values differ 10-20% from the modeled values. These discrepancies maybe due to unmodeled partial blocking of groundwaves by terrain during the day and the fact that the space constants associated with PacNet and NLDN sensors differ. As the geometry of the network evolves with the addition of new sensors, network DE and LA will be reevaluated in future.

2. Relationships between lightning, precipitation, and hydrometeor characteristics over the North Pacific Ocean

Lightning data from the PacNet/LLDN and Lightning Imaging Sensor (LIS) on the Tropical Rainfall Measurement Mission (TRMM) Satellite were compared to TRMM precipitation radar products and latent heating and hydrometeor data (Pessi and Businger 2008). Three years of data over the central North Pacific Ocean were analyzed. The data were divided into winter (October-April) and summer (June-September) seasons. During the winter, the thunderstorms were typically embedded in cold fronts associated with eastward propagating extratropical cyclones. Summer thunderstorms were triggered by cold upper-level lows associated with the tropical upper-tropospheric trough (TUTT).

Concurrent lightning and satellite data associated with the storms were averaged over 0.5˚ x 0.5° grid cells and a DE correction model was applied to quantify the lightning rates. The probability distribution function (PDF) for PacNet/LLDN lightning rate shows that the majority of the population is at the low end of the lightning rates (Fig. 7). Previous studies have shown similar cumulative distributions for oceanic lightning (Nesbitt et al. 2000; Petersen et al. 2005). The PDF for convective rainfall rate also shows an emphasis on the low end of the rainfall rates, although the slope of the curve is less steep than that of the lightning PDF (Fig. 7).

The results of the data analysis show a consistent logarithmic increase in convective rainfall rate with increasing lightning rates (Fig. 8). Moreover, other storm characteristics, such as radar reflectivity, storm height, IWP, and PWP show a similar logarithmic increase (e.g., Fig. 9). Specifically, the reflectivity in the mixed-phase region increased significantly with lightning rate and the lapse rate of Z decreased; both are well-known indicators of the robustness of the cloud electrification process. In addition, the height of the echo tops showed a strong logarithmic correlation with lightning rate. See Pessi and Businger (2008) for further details of the analysis and results.

Radar reflectivity increased throughout the troposphere with lightning rate. Specifically, the reflectivity in the mixed-phase region increased significantly with lightning rate and the lapse rate of Z decreased; both are well-known indicators of the robustness of the cloud electrification process (Fig. 9). In addition, the height of the echo tops showed a strong logarithmic correlation with lightning rate.

A similar slope in the lightning-convective rainfall relationship for both summer- and winter cases indicate that over the central North Pacific, the average lightning-rainfall relationship is relatively independent of the season and storm type. Stratiform rain rate, however, was poorly correlated with lightning and remained nearly constant despite of the lightning rate.

Logarithmic and exponential distributions, such as those found the in analysis presented here, commonly occur in the atmosphere. The number density of the cumulus clouds has been observed to decrease nearly exponentially with increasing cloud size (e.g. Plank 1969). Drop-size distribution is exponential (Marshall and Palmer 1948), Junge et al. (1969) and Bullrich et al. (1966) studied aerosol distribution in Pacific airmasses and found sharp decay in the number of aerosol with aerosol radius. The distribution was approximated by a power law with an exponent between -3 and -4. Takahashi (1976), in a numerical study, found a logarithmic increase in rain rate when the number of cloud nuclei was decreased and approached a threshold value of ~150 cm^{-3}. Foster et al. (2003) found an exponential growth of rain rate with precipitable water in Hawaii.

Physically, the logarithmic relationship between lightning and convective rainfall can be interpreted in the following way. Assuming some CAPE and low-level moisture convergence over a limited area, a cloud starts to grow and the rainfall production is initiated relatively “easily”. The number of CCN has a great impact on the precipitation initiation and development (e.g. Takahashi 1976; Göke 2007), but assuming relatively uniform aerosol content over the ocean, the available moisture content determines the maximum potential rainfall rate. Other environmental conditions have weaker impact on the rainfall rate.

In contrast, the requirements for a robust charge-separation process are much more complex. Updraft speed, supercooled liquid water content, and ice content all need to be sufficient at the right altitude within a cloud. Other, yet to be defined, conditions may also play a role. Although weak cloud electrification is fairly common, the highest potential lightning rates are observed only on rare occasions when all the conditions for active lighting are met in a complex convective system.

These environmental circumstances and the results presented here suggest that the estimation of, for instance, rainfall rates from lightning rates is relatively insensitive at high lightning rates and more sensitive at low lightning rates. This is an encouraging result for lightning data assimilation applications, since the areas of strong storm activity and high rainfall rates, although less common, are the most important for NWP modeling.

3. Applications of PacNet/LLDN datastream

The results of the analysis effort over the North Pacific Ocean provide evidence that the lightning-rainfall relationship is relatively robust over the central-north Pacific Ocean (Pessi and Businger 2008). These results suggest that the data from PacNet/LLDN can be used as a proxy to estimate convective rainfall, latent heating, and hydrometeor profiles from lightning rates over the open ocean.

Several studies have shown that lightning data can be assimilated into numerical models to help to improve the model forecasts (Alexander et al 1999; Chang et al. 2001; Papadopoulos et al. 2004; Pessi et al. 2006). The lack of in situ data over the Pacific Ocean for initializing numerical models can lead to large forecast errors for storms that impact the west coast of North America or Hawaii.

In this study, lightning data was assimilated into MM5 using a latent heating adjustment method (e.g. Manobianco et al. 1994). The method adjusts model's latent heating rates depending on the lightning rates at each grid point. The adjustment is performed at every model time step during the first eight hours of the model integration. An empirical lightning-rainfall relationship (Pessi and Businger 2008) was used to convert the PacNet lightning rates to rainfall rates.

The assimilation technique was implemented in the Kain-Fritsch convective parameterization scheme. The method scales the model's vertical latent heating profiles at each grid point and model level depending on the ratio between rainfall predicted by the model and rainfall derived from lightning data. Scaling is done only if the observed rain rate (derived from lightning) is greater than the model produced rain rate. To prevent excessive latent heating values and model instability, the scaling coefficient was limited to three. If the observed rain rate was zero, no assimilation was done, as the absence of lightning does not imply the absence of rain. If the rain rate derived from lightning observations at any grid point was greater than zero, but the model rain rate was zero, a search algorithm was used. Initially the algorithm searches the adjacent model grid points for similar rainfall rates as those observed. Further grid points are gradually included in the search until a match is found. After the match is found, the vertical latent heating profile from the matching grid point is used and the levels where the heating rate is positive are saturated.

A poorly forecast mid-latitude cyclone that approached the west coast of the United States was simulated using available LLDN data. Beginning on 16 December 2002, this extratropical cyclone produced a large amount of lightning as it moved across the eastern North Pacific Ocean. On December 18, the center of the storm was located near 43˚ N latitude and 135˚ W longitude, northeast of Hawaii and west of Oregon. Most of the lightning activity was associated with the cold front (Fig. 10).

The surface analysis showed a storm central pressure of 972 hPa at 12 UTC on 19 December, whereas the operational NCEP Eta run was 11 hPa too high, and the MM5 control forecast was 10 hPa too high (Fig. 11a). When lightning data were assimilated, the storm deepened rapidly after the initialization and reached 974 hPa at 12 UTC (Fig. 11b). The increase in rainfall rates, with lightning data assimilation, occurred mostly near the cold front and in the trailing cold pool (Fig. 12). The pressure dropped further 2 hPa and reached 972 hPa at 15 UTC (Fig.13).

4. Summary and Conclusions

Thunderstorms pose a variety of hazards to aviation and marine interests, including high winds, wind shear, microbursts, turbulence, icing, heavy precipitation, and lightning strikes. In remote regions where conventional weather data are sparse and satellite data are either infrequent or unrevealing, tracking of thunderstorms, squall lines, and developing cyclones are important challenges in weather prediction for civilian and military purposes. Long-range lightning data from PacNet/LLDN are useful for a variety of nowcasting and forecasting applications including (i) planning of trans-oceanic flight routes and in development of optimum ship tracks for ocean voyages, (ii) estimating convective rainfall, latent heating, and hydrometeor profiles from lightning rates over the open ocean, (iii) evaluating the current intensity and near-term potential for intensification in tropical and extratropical cyclones, and (vi) assimilation in NWP models to improve numerical forecasts.

Long-range lightning sensors represent a mature, low-maintenance technology. Given the promising results obtained to date through analysis of the PacNet/LLDN data stream (e.g., Squires and Businger 2008; Pessi et al. 2008; Pessi and Businger 2008), plans are being developed for Pacific-wide coverage by an expanded network of sensors. Additional sensors will increase overall detection efficiency, while improving the location accuracy of an expanded PacNet/LLDN.

7. Acknowledgments

We are grateful to James Weinman for his encouragement to undertake the development of PacNet, to Joseph Nowak for help with detector site selection and installation, and to Nancy Hulbirt for assistance with graphics. This work is supported by the Office of Naval Research under grant number N000140510551.

REFERENCES

Alexander, G. D., Weinman, J. A., Karyampudi, V. M., Olson, W. S., and Lee, A. C. L., 1999: The Effect of Assimilating Rain Rates Derived from Satellites and Lightning on Forecasts of the 1993 Superstorm. *Mon. Wea. Rev.*, 127, 1433-1457.

Bullrich, K., R. Eiden, R. Jacnicke, and W. Nowak, 1966: Optical transmission of the atmosphere in Hawaii, *II. Final Tech. Rept.*, J. Gutenberg U., Mainz, Germany, Contract No. DA-91-591-EUC-3458, 3479 pp.

Chang, D-E., J. A. Weinman, C. A. Morales, and W. S. Olson, 2001: The Effect of Spaceborne Microwave and Ground-Based Continuous Lightning Measurements on Forecasts of the 1998 Groundhog Day Storm. *Mon. Wea. Rev.*, 129, 1809-1833.

Cummins K.L., M. J. Murphy, E. A. Bardo, W. L. Hiscox, R. D. Pyle, and A. E. Pifer, 1998: A combined TOA/MDF technology upgrade of the U.S. National Lightning Detection Network. *J. Geophys. Res.,* 103, 9035-9044.

Demetriades, N.W.S. and R.L. Holle, 2005: Long-range lightning applications for hurricane intensity and precipitation nowcasting. *Preprints, Conf. on Meteor. Appl. of Lightning Data*, San Diego, California, Jan. 9-13, Amer. Meteor. Soc., 9 pp.

Futyan, J. M., and A. D. Del Genio, 2007b: Relationships between lightning and properties of convective cloud clusters, *Geophys. Res. Lett.*, 34, L15705, doi:10.1029/2007GL030227.

Göke, S., H.T. Ochs, and R.M. Rauber, 2007: Radar Analysis of Precipitation Initiation in Maritime versus Continental Clouds near the Florida Coast: Inferences Concerning the Role of CCN and Giant Nuclei. *J. Atmos. Sci.*, 64, 3695–3707.

Junge, C. E., E. Robinson, and F. L. Ludwig, 1969: A Study of Aerosols in Pacific Air Masses. *J. Appl. Meteor.*, 8, 340-347.

Manobianco, J., S. Koch, V.M. Karyampudi, and A.J. Negri, 1994: The Impact of Assimilating Satellite-Derived Precipitation Rates on Numerical Simulations of the ERICA IOP 4 Cyclone. *Mon. Wea. Rev.*, **122**, 341–365.

Marshall, J. S., and W. M. Palmer, 1948: The distribution of raindrops with size. *J. Atmos. Sci.*, 5, 165-166.

Nesbitt, S. W., E. J. Zipser, and D. J. Cecil, 2000: A Census of Precipitation Features in the Tropics Using TRMM: Radar, Ice Scattering, and Lightning Observations. *J. Climate*, 13, 4087–4106.

Papadopoulos, A., T. Chronis and E. N. Anagnostou, 2005: Improving Convective Precipitation Forecasting Through Assimilation of Regional Lightning Measurements in a Mesoscale Model. *Mon. Wea. Rev.,* 133, 1961-1977.

Pessi A. and S. Businger, 2008: Relationships Between Lightning, Precipitation, and Hydrometeor Characteristics over the North Pacific Ocean. *J. Appl. Meteor.* (In review).

Pessi, A., S. Businger, and T. Cherubini, 2006: Comparison of two Methods for Assimilation of Lightning Data into NWP Models. *Preprints, 1st International Lightning Meteorology Conference*, Tucson, Arizona, 26-27 April 2006.

Pessi A., S. Businger, K. L. Cummins, N. Demetriades, M. Murphy, and B. Pifer, 2008: Development of a Long-Range Lightning Detection Network for the Pacific: Construction, Calibration, and Performance. *J. Atmos. Oceanic Technol.* (In review).

Petersen, W. A., H. J. Christian and S. A. Rutledge, 2005: TRMM observations of the global relationship between ice water content and lightning, *Geophys. Res. Lett.*, 32, No. 14, L14819 10.1029/2005GL023236.

Plank, V. G., 1969: The Size Distribution of Cumulus Clouds in Representative Florida Populations. *J. Appl. Meteor.*, 8, 46-67.

Squires, K., and S. Businger, 2008: The Morphology of Eyewall Lightning Outbreaks in Two Category Five Hurricanes. *Mon. Wea. Rev.* In press.

Takahashi, T., 1976: Warm Rain, Giant Nuclei and Chemical Balance: A Numerical Model. *J. Atmos. Sci.*, 33, 269-286.

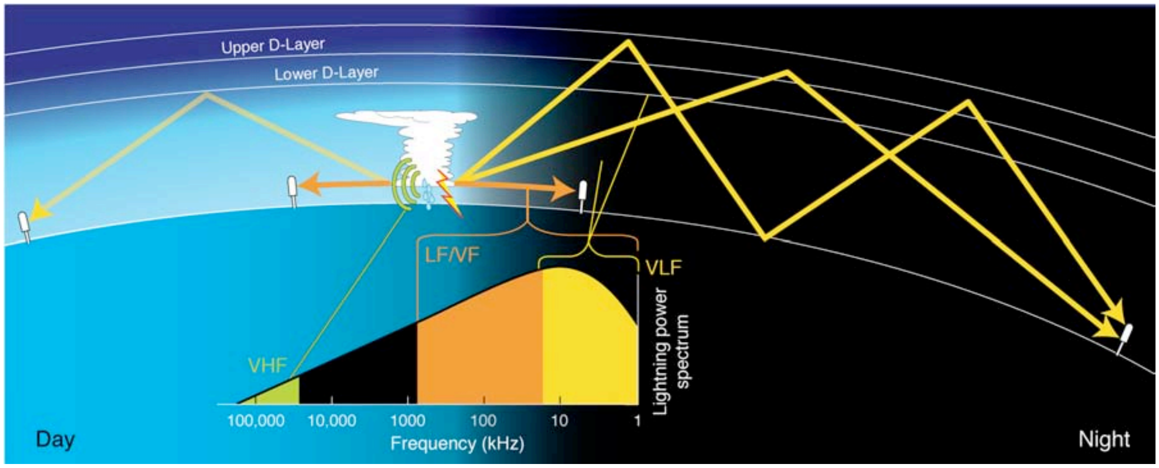

Fig. 1 Schematic diagram of the Earth-ionosphere wave-guide, which allows VLF (3-30 kHz) emissions from thunderstorms (sferics) to propagate thousands of kilometers through reflection. The best propagation is observed over the ocean at night.

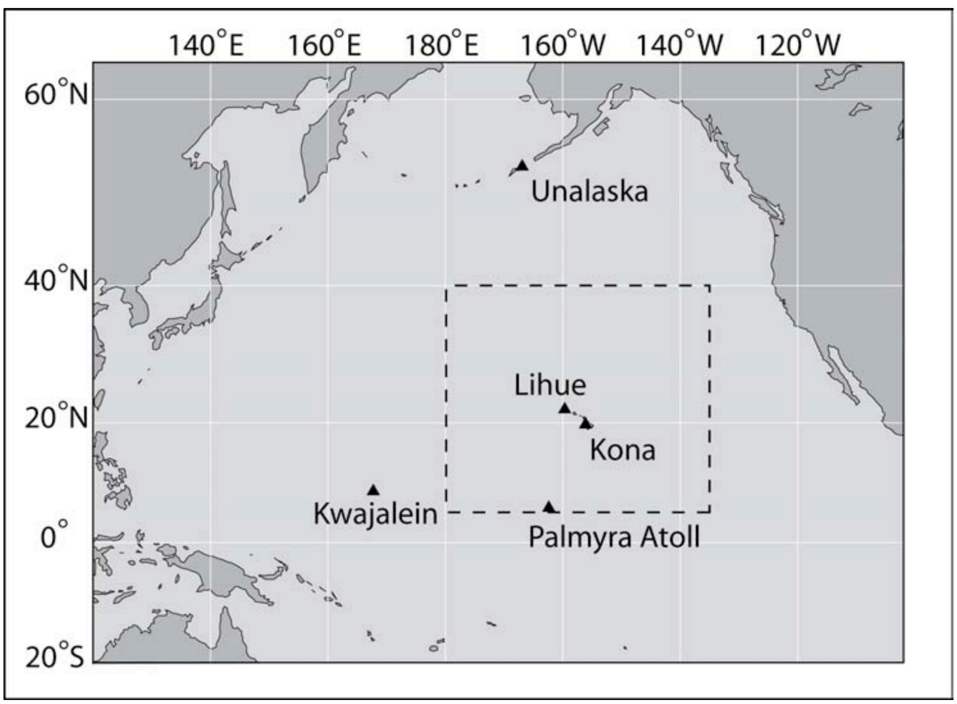

Fig. 2 Four sensors have been installed at Unalaska, Lihue, Kona and Kwajalein. The long-range lightning detection network (LLDN) sensors installed in the North America contribute specifically over the eastern Pacific. Dotted rectangle shows the area of analysis for the lightning-hydrometeor comparisons discussed in section 3.

Fig. 3 Roof installation in Unalaska.

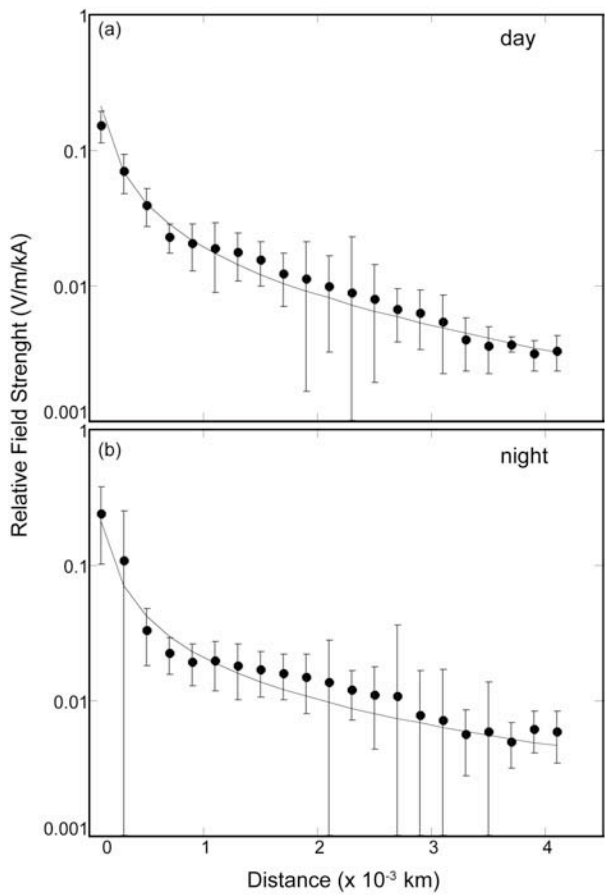

Fig. 4 Relative signal strength as a function of stroke distance as detected by a PacNet test sensor located in Tucson, Arizona for (a) day and (b) night. The error bars are ±1 standard deviation.

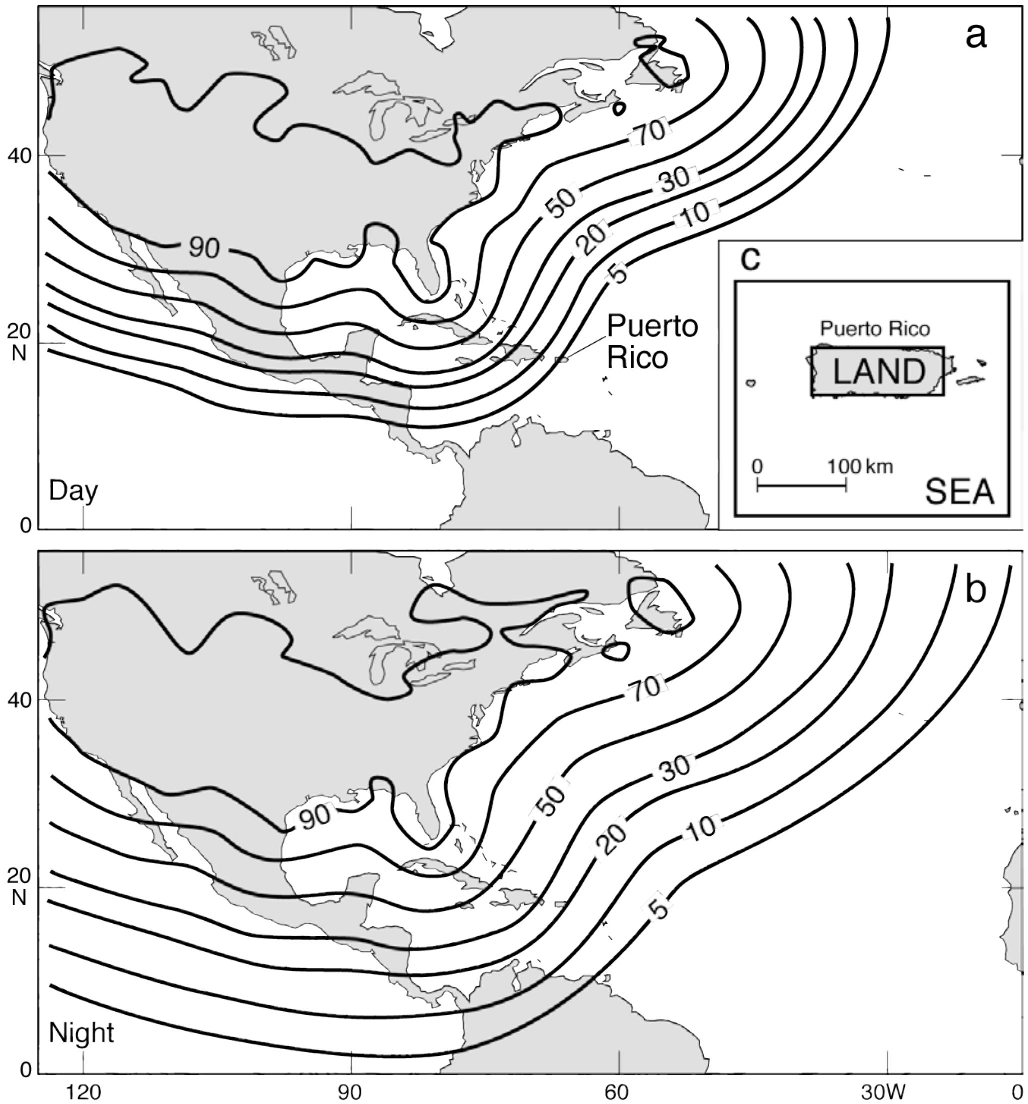

Fig. 5 Results from the detection efficiency model show (a) 5% day and (b) 20% night DE over Puerto Rico when using the reference peak-current distribution and space constants of 2000 and 6000 km for day and night, respectively. (c) Insert: Lightning data analysis region for Puerto Rico. The salt-water region is the “Sea” region, with the exclusion of the “Land” region.

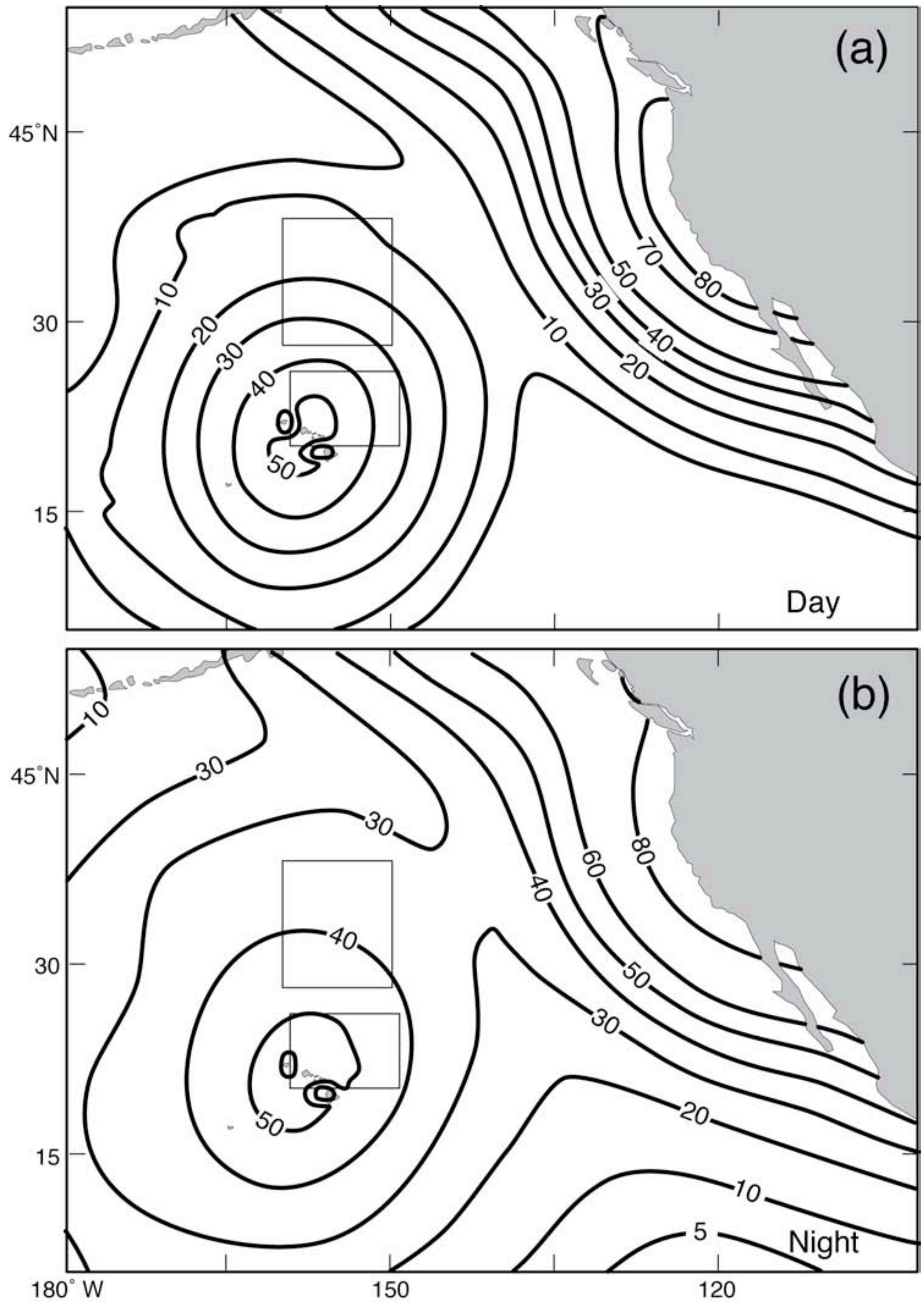

Fig. 6 Modeled DE (%) over the Pacific during a) day, and b) night. The boxes show the areas where the observed DE was assessed. The observed values for the Hawaii region were 22% and 61% during the day and night, respectively. DE values for the central-north region were 19% and 44% for day and night, respectively.

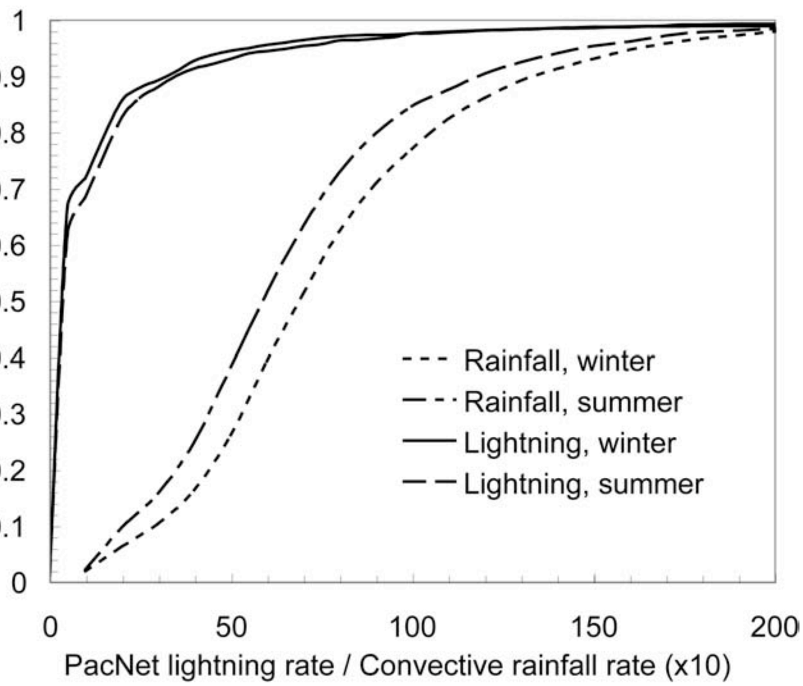

Fig. 7 Probability distribution function for PacNet/LLDN lightning rate [flashes × (10^4 km^2 h^{-1})$^{-1}$] and PR convective rainfall rate [mm h^{-1} × 10]. The x-axis is suppressed with ~99% of the highest rates shown.

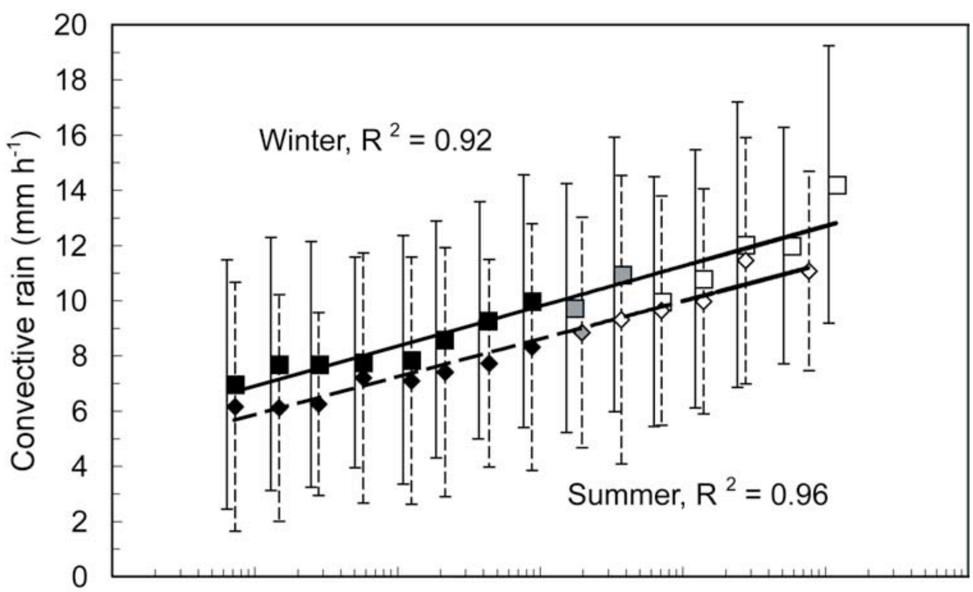

Fig. 8 Convective rainfall vs. lightning rate. Squares and solid lines are for winter data and diamonds and dashed lines for summer data. Filled symbols are PacNet/LLDN data, open symbols are LIS data, and grey symbols are combined PacNet/LLDN and LIS data. Abscissa shows the number of lightning flashes per hour normalized over 10^4 km^2. The error bars are ± 1 σ.

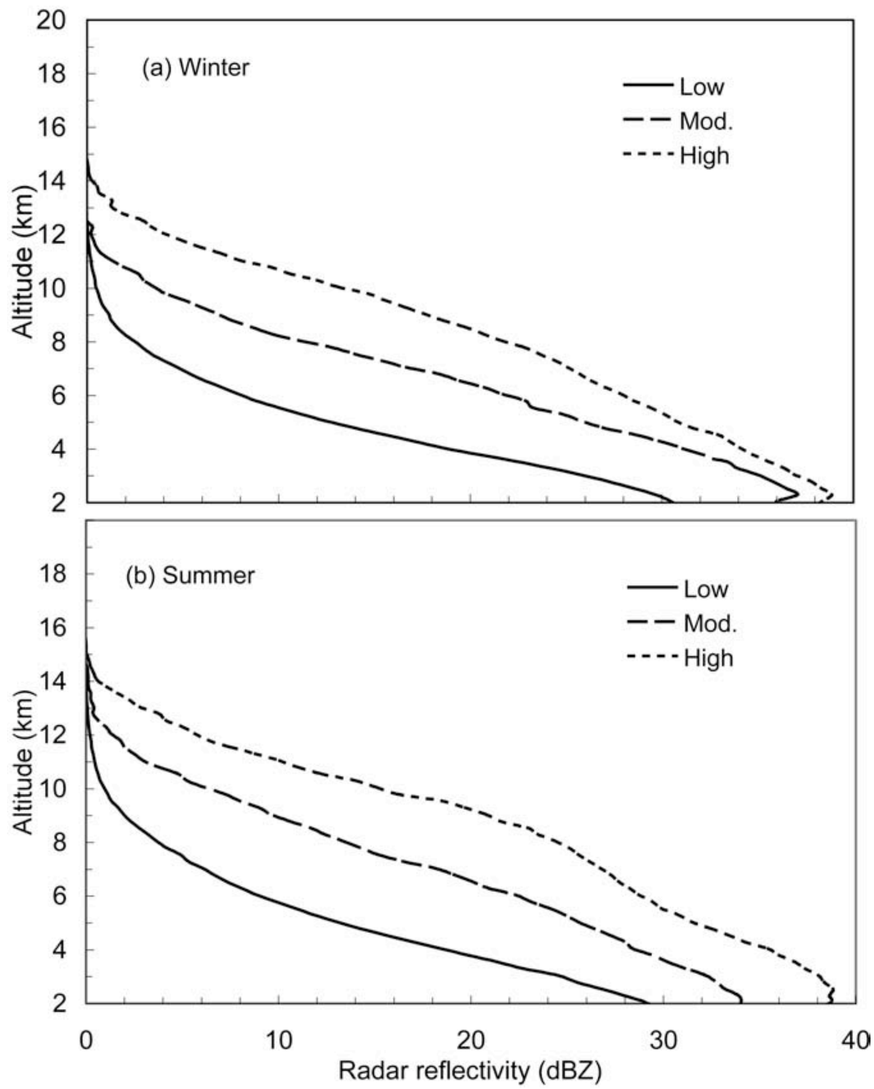

Fig. 9 Vertical profiles of PR reflectivity in (a) winter and (b) summer for three different lightning rate categories (low, moderate, and high lightning rate). Low lightning rate category is the lowest bin from PacNet/LLDN data, moderate category is the highest PacNet/LLDN data bin, and high category the highest LIS bin, as described in section 2c. Lowest levels are not shown since the near surface range bins were frequently filled with surface clutter, or missing data. Despite a sensitivity threshold for PR echos of ~17 dBZ, values start from zero because of the compositing method.

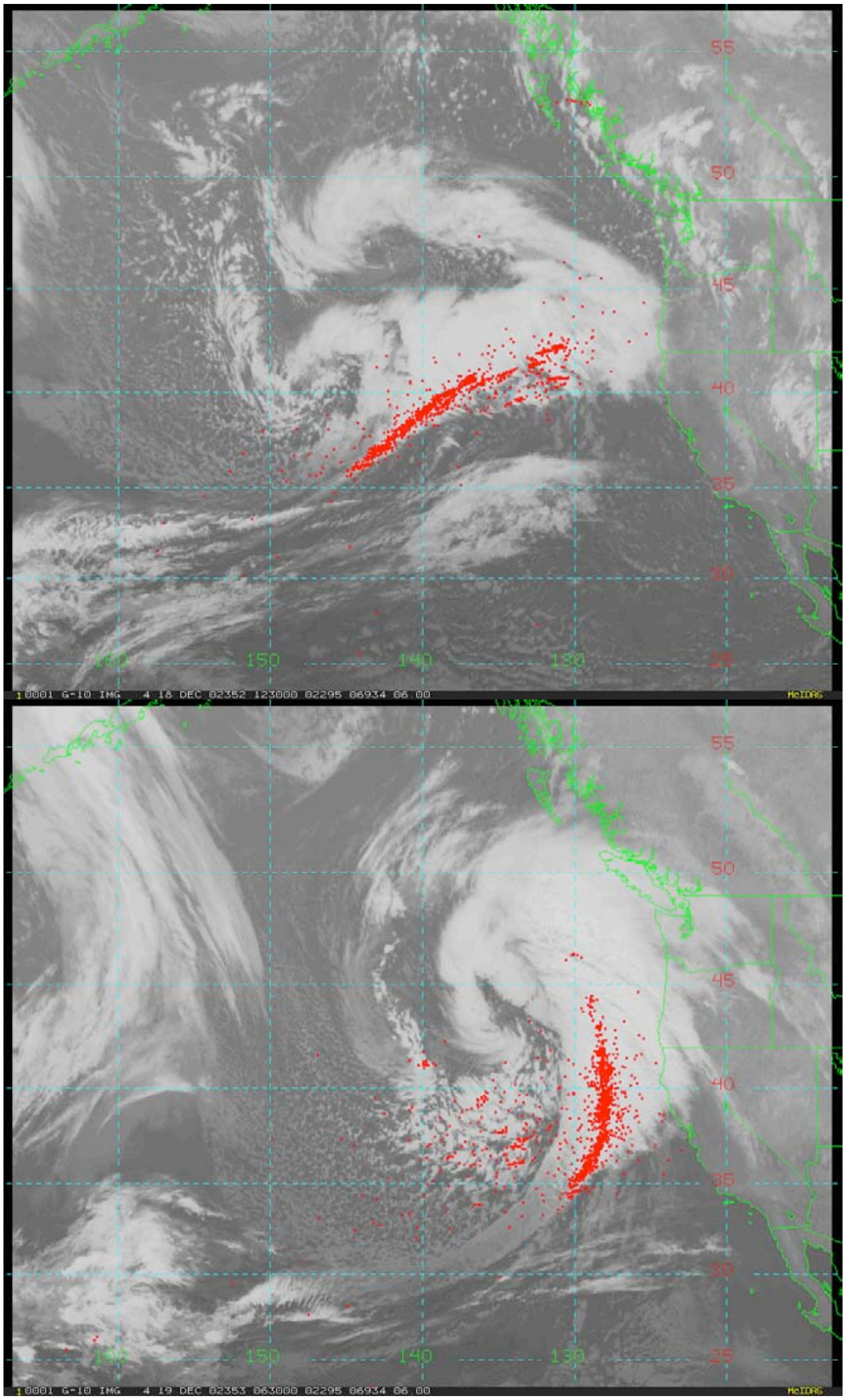

Fig. 10 A strong winter storm over the eastern Pacific Ocean at (a) 1230 UTC on 18 December 2002 and (b) 0630 UTC on 19 December 2002. Long-range lightning data (red dots) occurring ± 30 min. of the time of the image are overlaid with GOES-10 infrared satellite images.

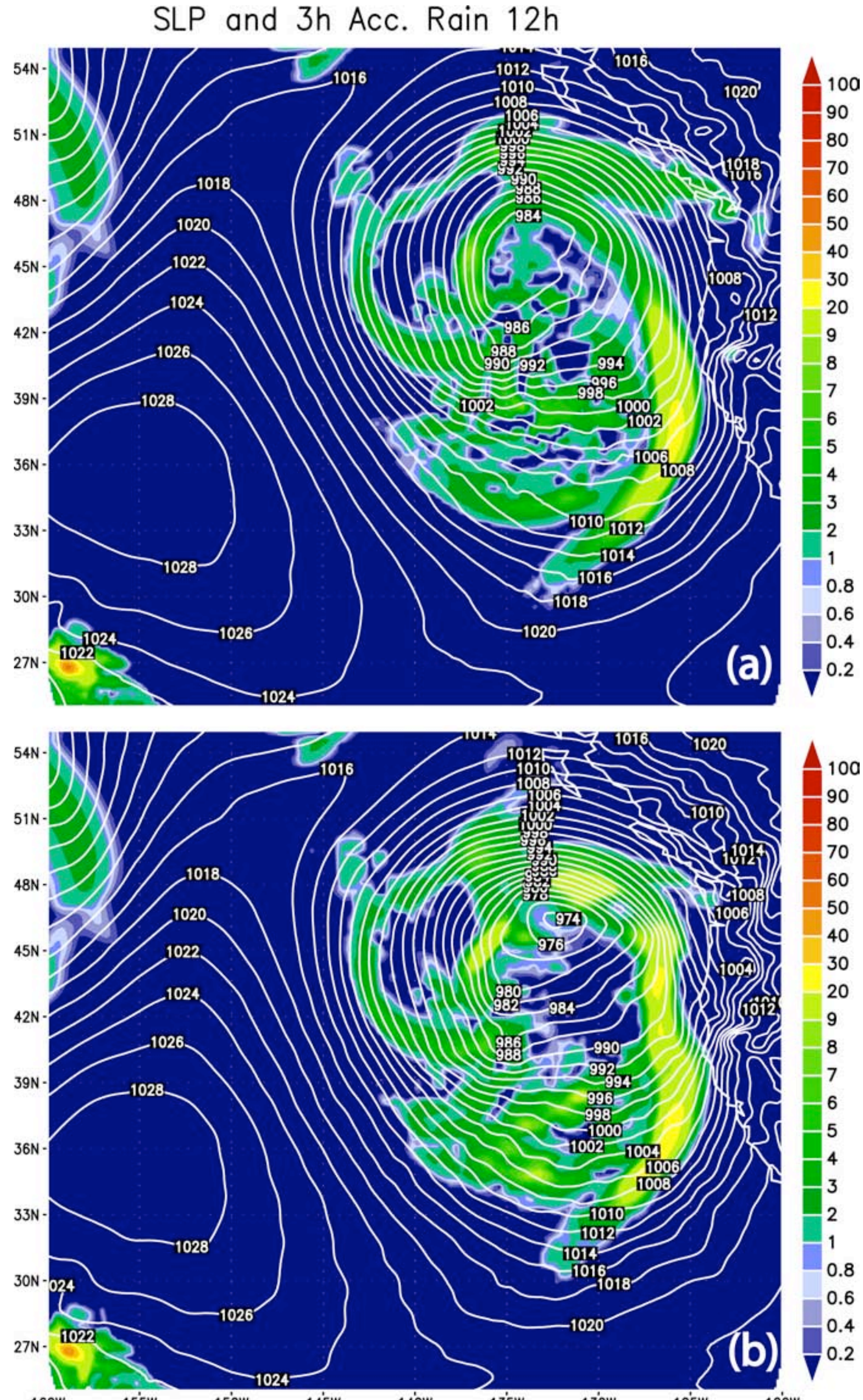

Fig 11 Twelve-hour MM5 forecast of sea-level pressure (hPa) and accumulated rainfall (mm) valid at 1200 UTC on 19 December 2002. (a) Without (control run) and (b) with lightning data assimilation.

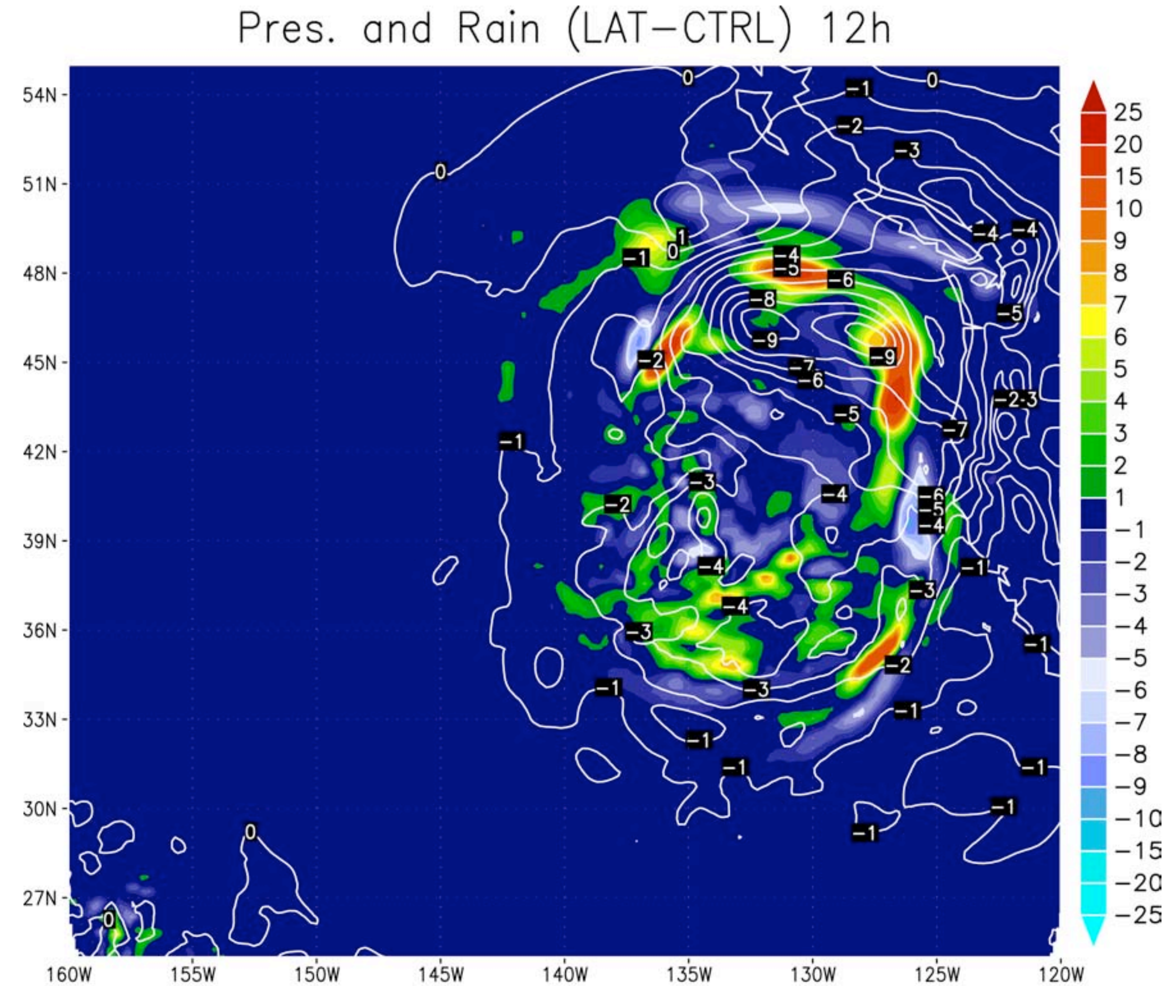

Fig. 12 The difference in sea-level pressure (hPa) and rainfall (mm) between the lightning data assimilation and control runs as shown in Fig. 11. Valid at 1200 UTC on 19 December 2002.

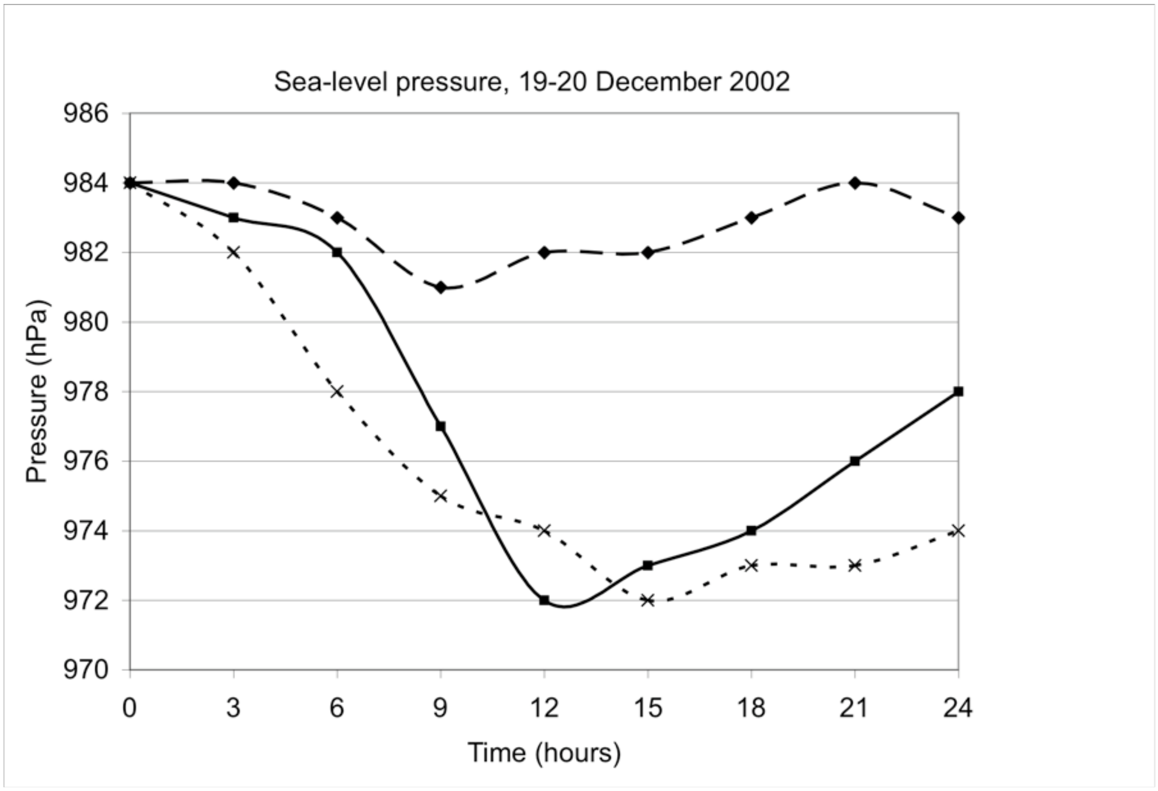

Fig. 13 Sea-level pressure over the North Pacific Ocean storm starting at 00 UTC on 19 December 2002. Minimum observed pressure was 972 hPa (solid), whereas control forecast was 10 hPa too high (dashed). Using lightning data assimilation (dotted), the central pressure dropped within 1-2 hPa of the observed value.